THE BALTIC JOURNAL
OF ROAD
AND BRIDGE
ENGINEERING
2023/18(3)

ISSN 1822-427X/eISSN 1822-4288
2023 Volume 18 Issue 3: 50–69
https://doi.org/10.7250/bjrbe.2023-18.608

MULTI-SCALE DECAY MECHANISM OF EMULSIFIED ASPHALT COLD RECYCLED MIXTURE UNDER FREEZE-THAW

YANHAI YANG*[1], LIANG YUE[1], YE YANG[1,2], GUANLIANG CHEN[1]

[1]*School of Transportation and Geomatics Engineering, Shenyang Jianzhu University, Shenyang, China*

[2]*College of Transportation Engineering, Dalian Maritime University, Dalian, China*

Received 25 December 2022; accepted 28 March 2023

Abstract: The road performance decay law of EACRM under freeze-thaw cycles was studied using laboratory tests on the macroscopic scale in order to comprehensively analyze the serious performance damage mechanism of emulsified asphalt cold recycled mixture (EACRM) in cold regions during the service period. The surface cracking behavior, internal void evolution characteristics, and asphalt mortar morphology damage of EACRM under freeze-thaw cycles were studied by means of digital speckle, industrial CT, and scanning electron microscope (SEM) on the mesoscopic and microscopic scale. The results show that along with the increase in the number of freeze-thaw cycles, the road performance of EACRM decreases significantly. The surface of EACRM obviously cracks, and the width and number of main cracks increase significantly. The fatigue times of the maximum horizontal strain in the whole field gradually decrease. Air voids and the average volume of meso-void visibly

* Corresponding author. E-mail: YHYang@sjzu.edu.cn

Yanhai YANG (ORCID ID 0000-0002-1599-7873)
Liang YUE (ORCID ID 0000-0002-2934-7572)
Ye YANG (ORCID ID 0000-0002-3897-6274)
Guanliang CHEN (ORCID ID 0009-0007-5394-3909)

increase. The microcracks of cement-emulsified asphalt mortar constantly emerge at the interface. The serious damage of the "three-dimensional network structure" is the fundamental reason for the performance decay of EACRM in cold regions. The performance damage of EACRM in cold regions is aggravated by water seeping into voids from cracks. Eventually, EACRM shows serious freeze-thaw inflicted damage.

Keywords: damage evolution behavior, emulsified asphalt cold recycled mixture (EACRM), freeze-thaw cycles, multi-scale research, road engineering, road performance decay.

Introduction

Emulsified asphalt cold recycled technology is an energy-saving, environment-friendly, green, and low-carbon solution. The emulsified asphalt cold recycled technology has the following advantages: high utilization rate of old materials, low energy consumption, low environmental pollution, and low cost. This technology has been widely used in road maintenance projects in China in recent years (Yang et al., 2023a, 2023b). However, EACRM still has some limitations related to air voids and water stability. In addition, due to the wide distribution of seasonal frozen areas in China (Yang et al., 2022a), severe freeze-thaw damage has occurred to EACRM serving in cold areas, limiting the application of emulsified asphalt cold recycled technology in seasonal frozen areas (Yang et al., 2022b). Therefore, the scientific problems of performance decay law and damage mechanism of EACRM under freeze-thaw need to be comprehensively studied.

At present, most of the research on ordinary asphalt mixture under freeze-thaw cycles is focused on volume parameters, road performance, mechanical properties, and damage models. It has been found that the closed air voids in asphalt mixture specimens after freeze-thaw increase by 20.3% (Wang et al., 2014). The internal voids of the mixture expand under freeze-thaw. Large voids are connected through separation voids, and new voids appear constantly (Xu et al., 2018), so more paths for water to move in the voids in the asphalt mixture appear (Gong et al., 2017). The water in the mixture may flow easier, which accelerates the water damage process of the asphalt mixture (Luo et al., 2018). In addition, road workers find that with the increase in the number of freeze-thaw cycles, the creep rate and dynamic stability of the asphalt mixture gradually decrease, the rutting depth gradually increases (Yang and Jiao, 2016), and the flexural and tensile strength and strain show a downward trend. The lower the freeze-thaw temperature, the greater the impact on low-temperature performance is (Duojie et al., 2021). With the increase in the number of freeze-thaw cycles, the internal friction angle increases, the compressive strength decreases, and the viscosity and cohesion gradually deteriorate. Thus, the structural integrity of the mixture is weakened and the ability to resist volume deformation is reduced. Finally, the loosening phenomenon is manifested (Yi et al., 2014), the fatigue resistance is obviously reduced (Guo et al., 2022), and the mechanical strength is obviously attenuated (Zheng et al., 2010; Ren et al., 2022). Wang et al. (2021) also discovered the decay mechanism of ordinary asphalt concrete, that is, the critical time for ordinary asphalt concrete to break increases with the increase of freeze-thaw cycles, the elastic modulus gradually decrease, the brittleness characteristics gradually increase, the toughness gradually decrease, the splitting strength gradually decreases, and the shear strength and flexural strength of ordinary asphalt concrete also decrease with the increase in the number of freeze-thaw cycles. A logistic damage model and a multivariate grey model were developed to simulate damage characteristics of the asphalt mixture under the action of freeze-thaw cycles considering the damage characteristics of the asphalt mixture (Wang et al., 2019). With the help of the reliability and damage theory, a three-dimensional model of freeze-thaw damage evolution of basalt fiber asphalt mixture was developed, and the improvement effect of the basalt fiber on frost-thaw resistance of the asphalt mixture was evaluated by enhancement factor (Cheng et al., 2019). A multi-scale model was designed based on thermodynamics, which could predict and reveal the evolution process of freeze-thaw damage of the asphalt mixture (Lövqvist et al., 2021). The fatigue-freeze-thaw unified equation of the asphalt mixture was developed based on the equivalent damage principle and direct correction method, which could better describe the coupling effect of freeze-thaw cycles and fatigue (Fan et al., 2020). Micro-cracks appear at the interface between asphalt and aggregate under freeze-thaw cycles. The cohesive force at the interface between asphalt and aggregate is lost, the internal gap is enlarged and connected, and the interfacial shear strength is reduced (Xu et al., 2020). These macro-performance studies have laid the foundation for the mesoscopic and microscopic scale research of asphalt mixtures under freeze-thaw. Adopting the non-contact digital image correlation (DIC) method to capture the Arcan fracture test process, Gao et al. (2014) assumed that the fracture path was dynamically selected. Wang et al. (2016) characterized the cracks of semi-circular specimens of the asphalt mixture on the micro-scale by DIC and found that the weak interface of the asphalt mixture was the most prone to cracking. In addition, on the mesoscopic scale, industrial CT scanning technology has been widely used in the research on blocking characteristics (Gu et al., 2021) and connected void characteristics (Xiao and Zhang, 2016) of drainage asphalt concrete, analysis of internal void distribution characteristics (Wu et al., 2012) of the asphalt mixture, uniformity evaluation (Guo et al., 2017), and air voids prediction (Guo et al., 2016). On the microscopic scale, the microstructure and chemical composition of the interface between cement asphalt mortar and cracks were analyzed by SEM and energy dispersive spectrometer (EDS) (Lin et al., 2020; Lyu et al., 2018). The adhesion between asphalt and aggregate was studied by atomic force microscope (AFM) and fluorescence spectrometer. The evolution of micro-characteristics of the mixture surface was monitored to evaluate the water damage resistance of the mixture (Yu and Zhou, 2021).

To sum up, these research results address the problem related to the indeterminate nature of the freeze-thaw damage mechanism of the ordinary asphalt mixture and provide reference and a wide range of research methods for the analysis of the freeze-thaw damage of EACRM. However, there are essential differences between EACRM and the ordinary asphalt mixture in terms of micro-mortar and interface, mesoscopic void characteristics, macro-material composition, and so on. It is difficult to directly apply the research results on freeze-thaw damage of the ordinary asphalt mixture to analyze the performance decay law and damage mechanism of EACRM under freeze-thaw cycles. In addition, previous research on freeze-thaw damage of the asphalt mixture often focused on the discussion of a single scale or comparison between two scales, and it is still necessary to further explore the freeze-thaw damage of EACRM on the multi-scale of "macro-meso-micro". Therefore, the road performance decay law, surface cracking behavior, mesoscopic void characteristics, and mortar morphology damage of EACRM under freeze-thaw cycles have been studied by macroscopic laboratory tests, digital speckle, industrial CT, SEM, and other microscopic test methods. Based on the multi-scale research results of "macro-meso-micro", the performance decay law and damage mechanism of EACRM in cold regions were systematically explained.

1. Materials and methods

1.1. Materials

EACRM is composed of reclaimed asphalt pavement (RAP), new aggregate, emulsified asphalt, cement, and water. RAP used in the study reflected in this paper is the milling material of first-class highway. In order to avoid the influence of RAP gradation variation on the test results, RAP was screened into 11 grades of single-size aggregates, including 16–19 mm, 13.2–16 mm, 9.5–13.2 mm, 4.75–9.5 mm, 2.36–4.75 mm, 1.18–2.36 mm, 0.6–1.18 mm, 0.3–0.6 mm, 0.15–0.3 mm, 0.075–0.15 mm, and 0–0.075 mm. Limestone alkaline aggregate was used as the new aggregate; it was also sieved into single particle size for use. In addition, 19–26.5 mm coarse aggregate missing in RAP screening was added to the new aggregate. Emulsified asphalt contained slow cracking cationic emulsified asphalt. The main performance test results of emulsified asphalt are shown in Table 1. In order to improve the early strength and service performance of EACRM, 1.5% 32.5# ordinary Portland cement was added during the test. The water used in the test was potable tap water. The materials used in this paper meet the requirements of the current relevant specifications effective in China.

Table 1. Test results of the emulsified asphalt

Test item	Test results	Technical requirement
Evaporation residue content, %	62	≥55
Sieve residue (1.18 mm sieve), %	0.029	≤0.1
Engla viscosimeter method E_{25}	7.4	2–30
Mixing test with coarse and fine aggregates	well-distributed	well-distributed
Storage stability at room temperature, % (1 d)	0.4	≤1
Storage stability at room temperature, % (5 d)	2.3	≤5

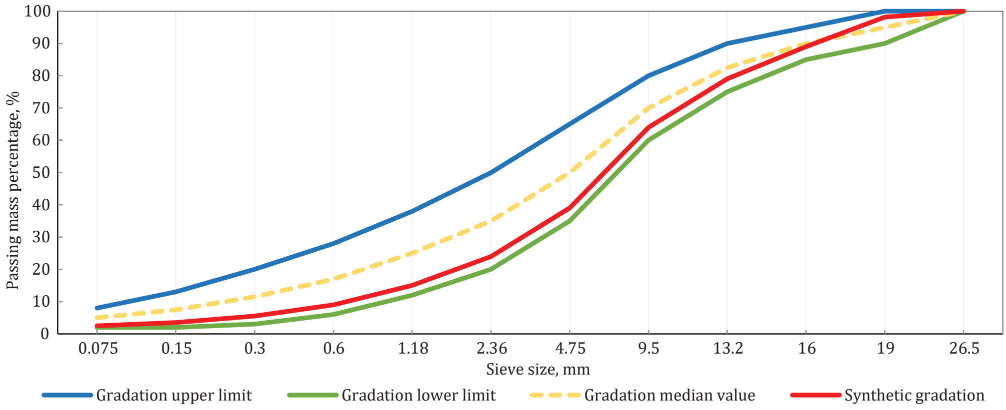

Figure 1. Gradation curve of EACRM

1.2. Gradation composition and mix proportion design

The gradation type of medium-grained EACRM was adopted in this paper, and the maximum nominal particle size was 19.0 mm. Firstly, the assessment of the mix proportion design of RAP and cement, new aggregate and cement should have been carried out according to the gradation requirements. The final synthetic gradation was obtained according to the mass ratio of 3:7. The gradation curve is shown in Figure 1. According to the Technical Specification for Highway Asphalt Pavement Recycling (JTG/T 5521-2019), the maximum dry density obtained by the hit test was used to determine the optimal moisture content of 3.0%. The optimal amount of emulsified asphalt was set at 3.5%, having determined the air voids, Marshall stability, 15 °C splitting strength, and the ratio of dry and wet splitting strength.

1.3. Experimental method

1.3.1. Freeze-thaw cycle test

The formed standard Marshall test specimens were subjected to vacuum water saturation treatment under the vacuum condition with the pressure of 98.3–98.7 kPa for 15 min. Then the specimens were taken out and put in a bag. 3–5 ml water was injected into the bag, which was sealed and put into the freeze-thaw circulation box. The freezing temperature was set to −20 °C and the melting temperature was set to 20 °C. The central temperatures of the test specimens were first reduced from room temperature to −20 °C and maintained for 1 h, then increased to 20 °C and maintained for 1 h. The heating and cooling rate was 1 °C/min. This process was defined as a freeze-thaw cycle. 0, 5, 10, 15, and 20 freeze-thaw cycles were performed, respectively. The subsequent test was conducted only after the specimens dried after the previous freeze-thaw cycle.

1.3.2. Macroscopic road performance

The high-temperature stability, low-temperature crack resistance, water stability, and fatigue performance of EACRM under freeze-thaw cycles were mainly studied. The high-temperature stability of EACRM was evaluated considering the penetration strength at 60 °C obtained from the uniaxial penetration strength test. The low-temperature crack resistance of EACRM was evaluated considering the −10 °C splitting tensile strength measured by the splitting test. The water stability of EACRM was evaluated considering the 15 °C splitting tensile strength measured by the immersion splitting test, the immersion splitting tensile strength, and the freeze-thaw splitting tensile strength ratio (TSR) measured by the freeze-thaw splitting strength test. The fatigue performance of EACRM was evaluated based on the indirect tensile fatigue test at 15 °C in the stress control mode. The termination condition of the fatigue loading test was that the specimens were completely broken or the fatigue times reached 10^5. The test stress ratios were 0.3, 0.4, and 0.5, respectively. A sinusoidal waveform with the loading frequency of 10 Hz was adopted. The axle load displacement load action times curve was recorded to obtain the fatigue times. The performance tests of EACRM specimens after 0, 5, 10, 15, and 20 freeze-thaw cycles, respectively, were carried out. Four parallel tests should have been conducted for each performance under different freeze-thaw times. After data processing, the average value was taken as the test result.

1.3.3. Surface cracking behavior

The cracking behavior of specimens under repeated loading was observed by Match ID three-dimensional digital speckle strain measurement and analysis system. In order to reduce the influence of rough specimen surface on the test results, Infra Test parallel double-sided cutting machine was used to flatten the specimen surface. The finished specimen was left standing at room temperature. After the specimen was completely dried, the cut side was sprayed with white spray paint to ensure that the spray paint evenly covered the specimen surface. After standing at room temperature until the surface spray paint was completely dry and hard, the speckles could be drawn. The special roller for digital speckles dipped in black ink was rolled on the test specimen sprayed with white paint until the specimen surface was evenly and randomly covered with black speckles. After the speckles dried, the test and observation could be carried out. The observation angle, height, distance, and light of the high-precision Match-ID three-dimensional digital speckle system were debugged before the test. Then the test could be carried out to photograph and collect the whole cracking process of the specimens. A strain nephogram of EACRM was obtained by digital speckle correlation method. The horizontal strains of the specimens under 0, 10, and 20 freeze-thaw cycles were analyzed. Then, the surface cracking behavior of EACRM under freeze-thaw was studied on the mesoscopic scale.

1.3.4. Mesoscopic void characteristics

The relative density of gross volume was measured by Corelok vacuum density tester. The theoretical maximum relative density was measured by vacuum method to calculate air voids of EACRM after 0, 10, and 20 freeze-thaw cycles, respectively. Industrial CT was used to scan the specimens that had undergone 0, 10, and 20 cycles of freeze-thaw. The specimens were fixed at the appropriate height of the mounting table. The crawler moving table was adjusted to ensure that the specimens were in the optimal position for X-ray scanning. The 3 mm copper-tin filter was placed, then the X-ray protection door was closed. Such parameters as energy, current, exposure time, and projection number were set by the control system before scanning started. X-ray CT scan images were preprocessed by Image J image processing software. The contrast of the image was adjusted. The effective part of the sample image was screened and intercepted by the interception tool to reduce the influence of noise on image quality. The processed images were imported and denoised by the Median Filter algorithm. The upper and lower surfaces of the specimens were partially cut off by Extract Subvolume. The specimens were intercepted by the Volume Edit function. The specimen images were processed by Interactive Thresholding. The void was separated and processed by Separate Objects. Finally, the mesoscopic void volume parameters were obtained. Then, the internal void decay characteristics of EACRM under freeze-thaw cycles were studied on the mesoscopic scale.

1.3.5. Microscopic morphological damage

The microscopic morphological damage of the emulsified asphalt cold recycled mortar under freeze-thaw was analyzed by SEM. The specimens after curing were crushed by the press at a constant rate. The relatively flat granular sample of asphalt mortar sheet was selected and placed in a dry and ventilated place to dry, and the non-conductive material was plated with gold. 10–15 gold-plated mortar sheets from the same sample were observed by SEM. The micromorphology of the emulsified asphalt composite mortar after 0, 10, and 20 freeze-thaw cycles was observed using Hitachi S4800 scanning electron microscope. Then, the morphology damage mechanism of asphalt mortar was revealed on the microscopic scale.

2. Results and discussion

2.1. Macroscopic road performance

The results of the uniaxial penetration strength test, splitting test, freeze-thaw splitting test, and fatigue life test of EACRM under freeze-thaw are shown in Figure 2(a) and Figure 2(b), respectively. The test specimens of EACRM after splitting test and freeze-thaw splitting test are shown in Figure 3(a) and Figure 3(b), respectively.

It can be seen from Figure 2 that the penetration depth of EACRM after 0 freeze-thaw cycle is 1.19 mm, the penetration strength is 1.07 MPa, the splitting tensile strength is 1.03 MPa, and the immersion splitting tensile strength is 0.70 MPa. However, after 20 freeze-thaw cycles, the penetration depth of EACRM increased to 1.65 mm, with a cumulative increase of 38.65%, the penetration strength decreased to 0.70 MPa, with a cumulative loss of 34.57%, the splitting tensile strength decreased to 0.56 MPa, with a cumulative loss of 45.78%, and the soaking splitting tensile strength decreased to 0.53 MPa, with a cumulative loss of 24.67%. At this time, the TSR is only 73.2%, lower than 75% of the specified value. From 0 to 20 freeze-thaw cycles, the fatigue life damage ratio of EACRM reached 53.5%, 66.5%, and 87.5%, respectively, when the stress ratio is 0.3, 0.4, and 0.5. This demonstrates that the high-temperature stability, low-temperature crack resistance, water stability, and fatigue performance of EACRM show a significant downward trend with the increase in the number of freeze-thaw cycles. In addition, the road performance decay of EACRM also shows a certain regularity. The loss of splitting tensile strength is most obvious during the 5th to 10th freeze-thaw cycles, the increase of penetration depth and strength loss are most obvious during the 10th to 15th freeze-thaw cycles, and the loss of immersion splitting tensile strength is most serious during the 15th to 20th freeze-thaw cycles.

It can be seen from Figure 3 that the appearance, failure form, and distribution of freeze-thaw test specimens after the split test are basically the same as those of the test pieces without freeze-thaw conditions. The failure forms are mainly manifested through cracks distributed along the radial direction, and each test specimen tends to be consistent. It indicates that the test specimen molding is relatively uniform and the variability is small. However, the cracks of freeze-thaw specimens are also accompanied by several branch joints, and the damage is more serious. This indicates that the freeze-thaw effect has a more significant impact on the strength attenuation of EACRM.

To sum up, it can be observed that the state of water in the void of EACRM changes due to freeze-thaw cycles. When water condenses into

(a) Results of road performance test

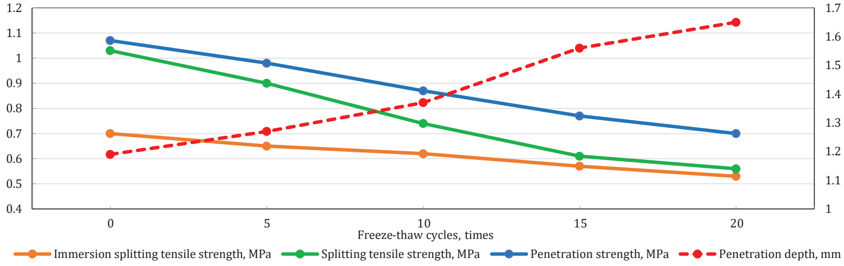

(b) Results of fatigue life test

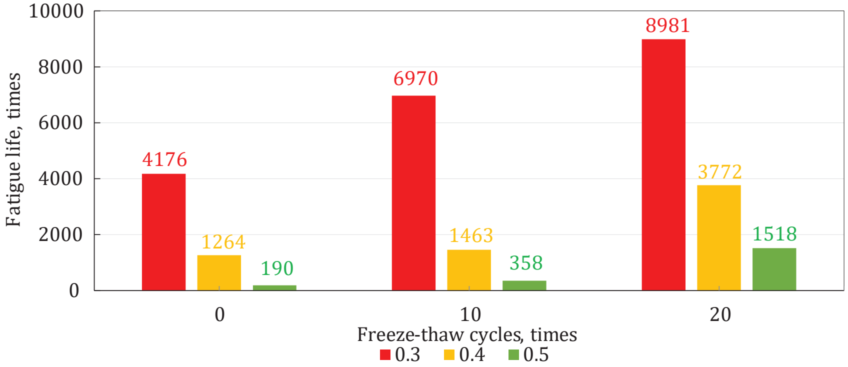

Figure 2. Results of macroscopic road performance

(a) A specimen after splitting test

(b) A specimen after freeze-thaw splitting test

Figure 3. Specimens after test

ice, its volume will expand abnormally. Temperature and frost heaving force are generated on the surface and inside of the mixture. Meso-void structure and micro-mortar morphology of the mixture are damaged. On the macroscopic scale, the surface of the mixture appears through cracks. Furthermore, the road performance of EACRM decreases greatly with the increase in the number of freeze-thaw cycles, this process is characterized by a certain regularity. Therefore, it is necessary to further analyze the surface cracking process of EACRM under freeze-thaw in order to reveal the freeze-thaw damage mechanism of EACRM on a mesoscopic scale.

2.2. Surface cracking behavior

In this paper, five test points have been obtained along the vertical centerline of the test specimen, which are represented by P1–P5, respectively, as shown in Figure 4. The average horizontal strain of each test point is extracted. The variation law between the number of fatigue actions N and the horizontal strain ε at each test point was analyzed. The horizontal strain in the local area of specimens with different freeze-thaw cycles was also analyzed. The horizontal strain of each test point is shown in Figure 5.

It can be seen from the results of different test points in Figure 5 that obvious strain concentration occurs at the center of each specimen, while the horizontal strain at the edge of the specimen is relatively small. This attests that the cracking behavior of EACRM under load is caused by the cracking and damage position in the middle which easily occur at earlier stages and gradually extends to both ends.

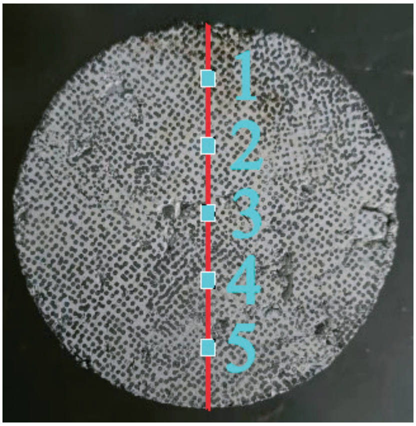

Figure 4. Test point distribution

It can be noticed considering the same color line in Figure 5 that the horizontal strain of each test point increases significantly in the middle and later stage of fatigue loading for the specimens with the same number of freeze-thaw cycles. Obvious cracking tendency was observed during the test. This allows noticing that the internal microcracks of EACRM accumulate continuously, and finally the cracking behavior is manifested on the surface.

It can be found from the same line type in Figure 5 that the fatigue times of the specimen with the full-field maximum horizontal strain in the same fatigue loading period gradually decrease with the increase in the number of freeze-thaw cycles and that the fatigue cycle is obviously shortened. It demonstrates that the larger the number of freeze-thaw cycles, the easier it is for EACRM to develop fatigue cracking in advance.

To sum up, the surface cracking behavior of EACRM is the accumulation of microcracks in the mixture at the early stage. The freeze-thaw cycle, as the "catalyst" of cracking and failure, accelerates

(a) 0 freeze-thaw cycles

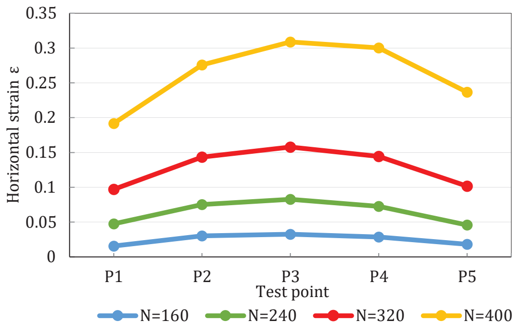

(b) 10 freeze-thaw cycles

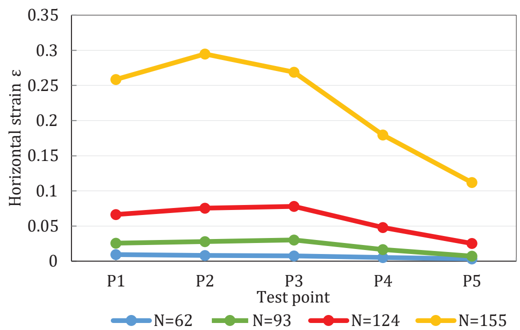

(c) 20 freeze-thaw cycles

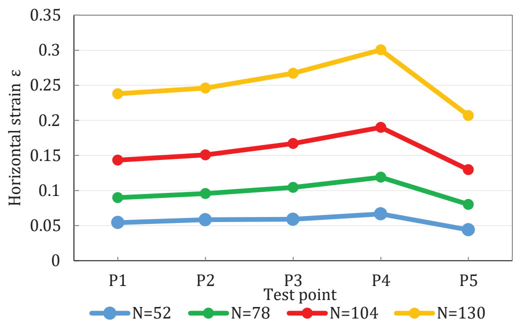

Figure 5. Horizontal strain of each test point under different freeze-thaw cycles

the damage to the strength of the meso-structure caused by temperature stress and frost-heaving force. In the middle and later periods, the surface of the final mixture cracked due to the destruction of the meso-void structure of the mixture. Therefore, it is necessary to further explore the decay law of mesoscopic void characteristics of EACRM.

2.3. Mesoscopic void characteristics

The air voids of EACRM under different freeze-thaw cycles are shown in Figure 6, the CT scanning image is shown in Figure 7, and the void volume distribution in Figure 8.

It can be seen from Figure 6 that the air voids of EACRM increased by 23.8% and 24.6%, respectively, from 0 to 10 freeze-thaw cycles and from 10 to 20 freeze-thaw cycles. This attests that with the increase of freeze-thaw cycles, the void fraction and growth trend of the specimens are significantly increased.

It can be seen from Figure 8 that the number and volume of voids in the range of 0–10 mm^3 and 10–100 mm^3 of EACRM specimen first increases and then decreases with the increase in the number of freeze-thaw cycles. However, the average volume of voids and the number and volume of voids in the range of 100–200 mm^3 increase with the increase of freeze-thaw cycles. In addition, in the range of 0–10 mm^3, the void volume distribution after 0, 10, and 20 freeze-thaw cycles is mainly concentrated in the range of 0–2 mm^3. In the range of 10–100 mm^3, the void volume after 10 and 20 freeze-thaw cycles increased sharply in the range of 15–35 mm^3 and 15–45 mm^3. In the range of 100–200 mm^3, the void volume after 0, 10, and 20 freeze-thaw cycles increased significantly in the ranges of 130–150 mm^3, 140–160 mm^3, and 140–170 mm^3. It shows that with the increase of freeze-thaw cycles, the mesoscopic void

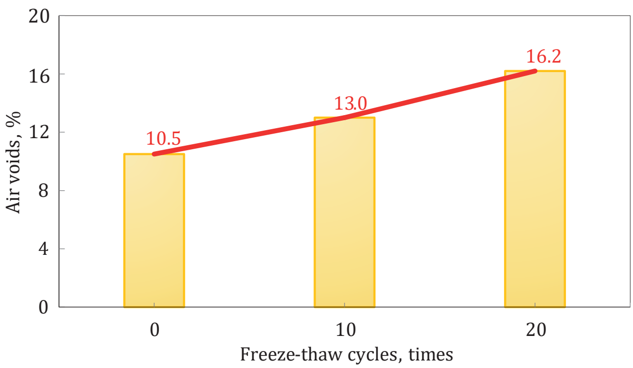

Figure 6. Air voids of EACRM under different freeze-thaw cycles

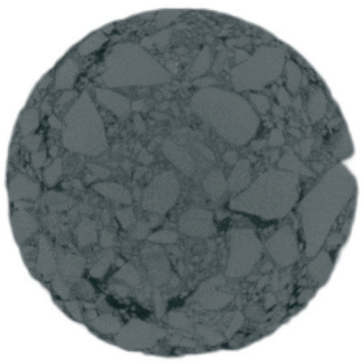

Figure 7. CT scanning image

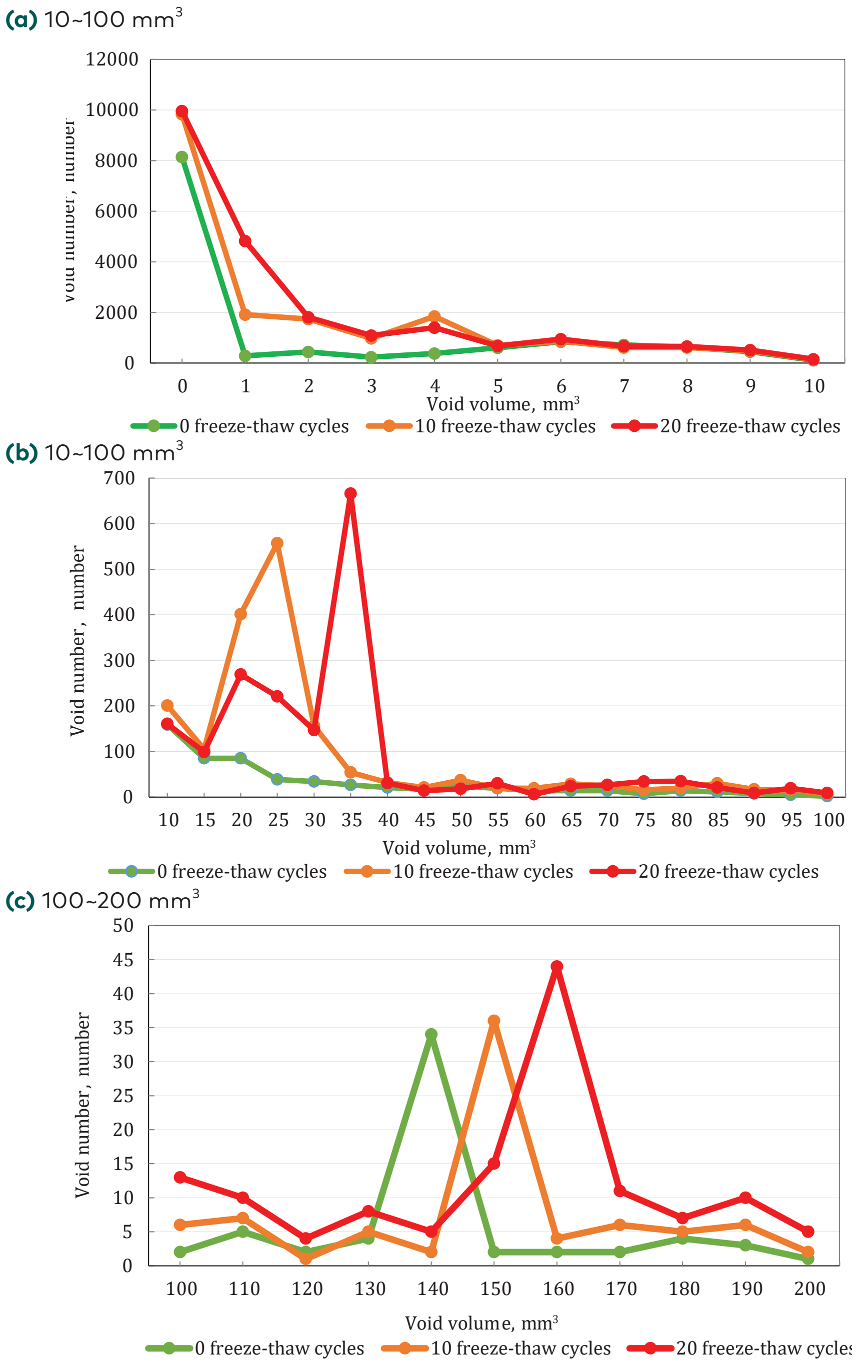

Figure 8. Void volume distribution of EACRM under different freeze-thaw cycles

of EACRM obviously increases, new voids keep sprouting, and the void volume obviously demonstrates a growing trend.

To sum up, the mesoscopic void characteristics of EACRM under freeze-thaw are void initiation, void expansion, and void penetration. A freeze-thaw cycle expands the volume of water in the void. The generated frost-heaving force expands the void volume, thus, more water enters the void and participates in the next freeze-thaw cycle. The frost-heaving force gradually increases with the increase of water content, and the continuous erosion of water inflow causes damage to asphalt mortar. With the increase in the number of freeze-thaw cycles, the bond strength of asphalt mortar gradually deteriorates, which leads to the continuous penetration of voids and accelerates the generation, expansion, overlapping, and penetration of micro-cracks. Finally, the decay of mesoscopic void characteristics and the appearance of surface cracking occur. Therefore, it is still necessary to study the microscopic morphology of asphalt mortar.

2.4. Microscopic morphological damage

The microscopic morphology of the cement emulsified asphalt mortar of EACRM after freeze-thaw for 0, 10 and 20 cycles was observed by SEM. The micro morphology of the cement emulsified asphalt mortar of cold recycled mixture under different freeze-thaw cycles is shown in Figure 9.

It can be seen from Figure 9(a) that after 0 freeze-thaw cycles, the cement hydration products of the cold recycled mixture of emulsified asphalt interlace in the form of needles and columns in the emulsified asphalt cement mortar on the aggregate surface. The relatively smooth asphalt on the aggregate surface becomes rough, and the connection between asphalt and hydration products is continuous, smooth

(a) 0 freeze-thaw cycles **(b)** 10 freeze-thaw cycles **(c)** 20 freeze-thaw cycles.

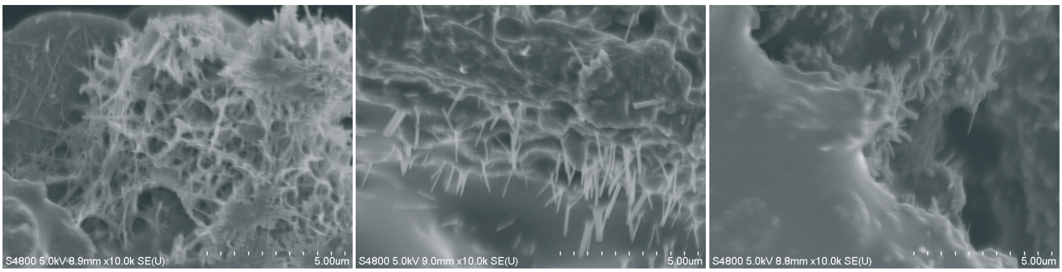

Figure 9. Micro-morphology of the cement emulsified asphalt mortar of the cold recycled mixture under different freeze-thaw cycles

and crack-free. A dense "three-dimensional network structure" is formed in the gap between the aggregates to connect and anchor. The reinforcement optimizes the microscopic spatial structure and improves the overall strength.

It can be seen from Figure 9(b) that after 10 freeze-thaw cycles, most of the cement hydration products change from coarse rods to fine needles. This demonstrates that the weak part of the cement emulsified asphalt composite mortar is washed by water during freeze-thaw cycles. The bond strength between the emulsified asphalt and cement hydration products is reduced, which makes the emulsified asphalt wrapped on the surface of the cement hydration product peel off. Eventually, the "three-dimensional network structure" got damaged.

It can be seen from Figure 9(c) that after 20 freeze-thaw cycles, the damage of the cement hydration products in the interface of the cement emulsified asphalt mortar is aggravated. A large amount of emulsified asphalt peels off from the surface of cement hydration products, and the number of hydration product crystals decreases, they become shorter and finer under the coupling effect of water scouring and frost-heaving force. Finally, the "three-dimensional network structure" was seriously destroyed, and the adhesive strength of asphalt mortar was lost.

In conclusion, with the increase in the number of freeze-thaw cycles, the crystal morphology of cement hydration products gradually degrades, the "three-dimensional network structure" of the cement emulsified asphalt mortar gradually deteriorates, and the adhesive strength of asphalt mortar is gradually lost. "Three-dimensional network structure" is the microscopic mechanism of the formation of the structural strength of EACRM. The structure of the cement emulsified asphalt mortar without freeze-thaw cycles is not damaged, which is the fundamental reason to ensure the performance of EACRM without freeze-thaw decay. Water erosion and the frost-heaving force generated by volume expansion are the direct reasons for the damage to the "three-dimensional network structure", and the freeze-thaw cycle is the main culprit responsible for the damage to the "three-dimensional network structure".

Conclusions

1. The high-temperature stability, low-temperature crack resistance, water stability, and fatigue performance of EACRM obviously deteriorate under freeze-thaw cycles. Moreover, the performance damage accumulates with the increase in the number of freeze-thaw cycles, and the mechanical strength is obviously lost in the later freeze-thaw cycles.

2. The "three-dimensional network structure" of the cement emulsified asphalt composite mortar is the microscopic structural strength mechanism of EACRM. The destruction of the "three-dimensional network structure" is the reason for the deterioration of the performance of EACRM in cold regions. Water erosion and the frost-heaving force generated by volume expansion are the main culprits that cause microscopic morphological damage and decay of void characteristics. Freeze-thaw cycles accelerate the damage of EACRM.
3. The freeze-thaw damage of EACRM first occurred in the microscopic cement emulsified asphalt compound mortar. With the increase in the number of freeze-thaw cycles, the micro "three-dimensional network structure" is gradually destroyed, the bonding strength of the asphalt mortar interface is significantly reduced, and the interface of cement emulsified asphalt mortar is damaged by microcracks. With the continuous initiation and expansion of microcracks, mesoscopic voids keep constantly emerging, expanding, overlapping, and penetrating. The air voids of the mixture increase significantly, and a large amount of water enters the void. The surface of the cold recycled mixture cracks obviously under the action of freeze-thaw cycle. The width and number of main cracks increase significantly. The surface of the specimens becomes rough and a small amount of fine aggregate falls off. Eventually, the road performance of EACRM is completely undermined.

Acknowledgments

The authors express their gratitude for the platform support provided by Shenyang Jianzhu University and would like to thank professors for their guidance in the process of conducting this research.

Funding

This study was supported by the National Natural Science Foundation of China [Grant No.52278454].

REFERENCES

Cheng, Y., Yu, D., Tan, G., et al. (2019). Evolution on freeze-thaw damage of basalt fiber asphalt mixture. *Journal of Harbin Engineering University*, *40*(3), 518–524.

Duojie, C., Si, W., Ma, B., Hu, Y., Liu, X., and Wang, X. (2021). Assessment of freeze-thaw cycles impact on flexural tensile characteristics of asphalt mixture in cold regions. *Mathematical Problems in Engineering*, *2021*, Article 6697693. https://doi.org/10.1155/2021/6697693

Fan, Z., Xu, H., Xiao, J., and Tan, Y. (2020). Effects of freeze-thaw cycles on fatigue performance of asphalt mixture and development of fatigue-freeze-thaw (FFT) uniform equation. *Construction and Building Materials*, *242*, Article 118043. https://doi.org/10.1016/j.conbuildmat.2020.118043

Gao, L., Ni, F., Braham, A., and Luo, X. (2014). Mixed-mode cracking behavior of cold recycled mixes with emulsion using Arcan configuration. *Construction and Building Materials*, *55*, 415–422. https://doi.org/10.1016/j.conbuildmat.2013.12.079

Gong, X., Romero, P., Dong, Z., and Li, Y. (2017). Investigation on the low temperature property of asphalt fine aggregate matrix and asphalt mixture including the environmental factors. *Construction and Building Materials*, *156*, 56–62. https://doi.org/10.1016/j.conbuildmat.2017.08.142

Gu, S., Chen, M., Lin, L., et al. (2021). Study on the clogging characterization of large void asphalt concrete. *Forest Engineering*, *37*(3), 126–130.

Guo, N., You, Z., Tan, Y., et al. (2016). Prediction method on volume of air voids of asphalt mixtures based on CT technique. *China Journal of Highway and Transport*, *29*(08), 12–21+42.

Guo, N., You, Z., Tan, Y., et al. (2017). Evaluation method for homogeneity of asphalt mixtures based on CT technique. *China Journal of Highway and Transport*, *30*(1), 1–9+55.

Guo, Z., Wang, L., Feng, L., and Guo, Y. (2022). Research on fatigue performance of composite crumb rubber modified asphalt mixture under freeze thaw cycles. *Construction and Building Materials*, *323*, Article 126603. https://doi.org/10.1016/j.conbuildmat.2022.126603

Lin, J., Huo, L., Xiao, Y., Xu, F., and Pan, P. (2020). Long-term performance characteristics and interface microstructure of field cold recycled asphalt mixtures. *Construction and Building Materials*, *259*, Article 120406. https://doi.org/10.1016/j.conbuildmat.2020.120406

Lövqvist, L., Balieu, R., and Kringos, N. (2021). Multiscale model for predicting freeze-thaw damage in asphalt mixtures. *International Journal of Pavement Engineering*, *23*(14), 5048–5065. https://doi.org/10.1080/10298436.2021.1991580

Luo, R., Liu, Z., Huang, T., et al. (2018). Effect of freezing-thawing cycles on water vapor diffusion in asphalt mixtures. *China Journal of Highway and Transport*, *31*(9), 20–26+64.

Lyu, Z., Shen, A., Qin, X., et al. (2018). Performance optimization and mechanism of emulsified asphalt cold recycled mixtures. *Journal of Building Materials*, *21*(4), 614–619.

Ren, M., Feng, H., Cong, L., et al. (2022). Strength evolution law and mechanism analysis of asphalt mixtures during water saturation. *Journal of Building Materials*, *25*(5), 537–544.

Wang, H., Zhang, C., Fang, J., et al. (2014). Study on low temperature performance and microstructure of rubber hot recycled mixture. *Journal of Hunan University (Natural Sciences)*, *41*(11), 123–128.

Wang, L., Gong, N., and Xing, Y. (2016). Characteristics of interface cracking for ultraviolet aged hot-mix asphalt based on digital speckle correlation method. *Acta Materiae Compositae Sinica*, *33*(4), 732–740. https://doi.org/10.13801/j.cnki.fhclxb.20150921.002

Wang, W., Cheng, Y., Ma, G., Tan, G., Sun, X., and Yang, S. (2019). Further investigation on damage model of eco-friendly basalt fiber modified asphalt mixture under freeze-thaw cycles. *Applied Sciences*, *9*(1), 60–75. https://doi.org/10.3390/app9010060

Wang, X., Zhang, X., Li, J., et al. (2021). Study on freeze-thaw fracture characteristics and damage mechanism of asphalt concrete. *Journal of Shenyang Jianzhu University (Natural Science)*, *37*(3), 518–527.

Wu, W., Wang, D., Zhang, X., et al. (2012). Air voids distribution of asphalt mixtures based on industrial computerized tomography. *Journal of Central South University (Science and Technology)*, *43*(6), 2343–2348.

Xiao, X., and Zhang, X. (2016). Research on connecting void characteristics of porous asphalt mixture based on industrial CT. *China Journal of Highway and Transport*, *29*(8), 22–28.

Xu, G., Yu, Y., Cai, D., Xie, G., Chen, X., and Yang, J. (2020). Multi-scale damage characterization of asphalt mixture subject to freeze-thaw cycles. *Construction and Building Materials*, *240*, Article 117947. https://doi.org/10.1016/j.conbuildmat.2019.117947

Xu, H., Li, H., Tan, Y., Wang, L., and Hou, Y. (2018). A micro-scale investigation on the behaviors of asphalt mixtures under freeze-thaw cycles using entropy theory and a computerized tomography scanning technique. *Entropy*, *20*(2), Article 68. https://doi.org/10.3390/e20020068

Yang, L., and Jiao, H. (2016). Study on rut test of asphalt pavement based on creep characteristics of freeze-thaw cycle. *Journal of China & Foreign Highway*, *36*(2), 69–73.

Yang, Y., Sun, Z., Yang, Y., Yue, L., and Chen, G. (2022a). Effects of freeze-thaw cycles on performance and microstructure of cold recycled mixtures with asphalt emulsion. *Coatings*, *12*(6), Article 802. https://doi.org/10.3390/coatings12060802

Yang, Y., Yue, L., Zhang, H., and Yang, Y. (2022b). Equivalent thickness coefficient of cold central plant recycling pavement structure. *Civil Engineering Journal*, *31*(2), 249–259. https://doi.org/10.14311/CEJ.2022.02.0019

Yang, Y., Yue, L., Cui, H., and Yang, Ye. (2023a). Simulation and evaluation of fatigue damage of cold recycled mixtures with bitumen emulsion. *Construction and Building Materials*, *364*, Article 129976. https://doi.org/10.1016/j.conbuildmat.2022.129976

Yang, Y., Yue, L., Yang, Y., et al. (2023b). Research on road performance prediction of cold recycled mixture under freeze-thaw based on ultrasonic method [J]. *Forest Engineering*, *39*(1), 140–148.

Yi, J., Shen, S., Muhunthan, B., and Feng, D. (2014). Viscoelastic plastic damage model for porous asphalt mixtures: Application to uniaxial compression and freeze thaw damage. *Mechanics of Materials*, *70*(3), 67–75. https://doi.org/10.1016/j.mechmat.2013.12.002